



The adsorption properties of biochar derived from woody plants or bamboo for cadmium in aqueous solution

Jian Wu^a, Dajun Ren^{a,b}, Xiaoqin Zhang^{a,b,*}, Zhihua Chen^c, Shuqin Zhang^{a,b}, Sheng Li^a, Linjun Fu^a

^aCollege of Resource and Environmental Engineering, Wuhan University of Science and Technology, Wuhan, 430081, China, email: 21640791142@qq.com (J. Wu), 2774276185@qq.com (S. Li), 2792472809@qq.com (L. Fu)

^bHubei Key Laboratory for Efficient Utilization and Agglomeration of Metallurgic Mineral Resources, Wuhan University of Science and Technology, Wuhan, Hubei 430081, China, email: 2dj_ren@163.com (D. Ren), Tel. +86 027-68862892, Fax +86 027-68862892, email: friedchickenlg@126.com (X. Zhang), 257791098@qq.com (S. Zhang)

^cSchool of Environment, Henan Normal University, Key Laboratory for Yellow River and Huai River Water Environment and Pollution Control, Xinxiang 453007, China, email: 2chenzhihua@htu.edu.cn (Z. Chen)

Received 10 September 2018; Accepted 27 March 2019

ABSTRACT

Biochar may potentially absorb heavy metals from aqueous solutions. In this study, biochar was derived from the pyrolysis (~600°C) of 11 plants that are widely distributed across the mid-west forest land of China. The three kinds of biochar with the highest cadmium (Cd) adsorption capacities were further investigated to establish their adsorption kinetics and isotherms. The results showed that biochar derived from walnut trees (W-Biochar), wild cherry trees (C-Biochar), and bamboo (B-Biochar) had the greatest adsorption capacity. Their order was B-Biochar (19.12 mg/g) > C-Biochar (18.8 mg/g) > W-Biochar (18.06 mg/g). The optimal biochar dosage was 2 g/L at pH = 5. A pseudo-second-order model explained the adsorption kinetics with rate constants of 0.043 g·mg⁻¹·min⁻¹ (B-Biochar), 0.321 g·mg⁻¹·min⁻¹ (C-Biochar), and 0.157 g·mg⁻¹·min⁻¹ (W-Biochar). It took 40 min to reach adsorption equilibrium, which was responsible for the Langmuir isotherm. The Fourier Transform Infrared spectrophotometer (FTIR) results showed that the hydroxyl and carboxyl groups on the biochar surface improved Cd²⁺ adsorption. The scanning electron microscope results showed that the three biochars had different microstructures, which were probably responsible for their different adsorption capacities.

Keywords: Biochar; Cadmium; Woody plants; Bamboo; Adsorption

1. Introduction

Cadmium (Cd) pollution has become a severe environmental issue in China and around the world. The Cd pollution is mainly caused by mining and smelting procedures, the over-use of chemical fertilizers and pesticides, and atmospheric deposition, etc. [1,2]. It has been reported that the Cd²⁺ has several adverse effects on human health, including damage to the liver, lungs, and bones, which may lead to severe diseases, such as cancer and other fatal

disorders [3]. Many methods have been used to remove Cd²⁺ from aqueous solutions, including chemical precipitation, membranes, and ion exchange and adsorption, etc. [4]. Among these methods, adsorption is widely adopted for the in-situ remediation of heavy metals in polluted soil because it is a low-cost method that is highly efficient and simple to operate [5].

Considerable attention has been paid to biochar, which is commonly derived from the pyrolysis of biomass, such as agricultural waste (chicken manure, pig manure, sawdust, straw, etc.), industrial organic waste, and urban sludge [6], etc. The biochar contains unique surface physicochemical

*Corresponding author.

properties (loose porosity and a large specific surface area with a variety of surface groups), which are useful for metal ions adsorption. Biochar has been shown to be very effective in immobilizing, adsorbing, and sequestering a number of heavy metals, such as lead (Pb), chromium (Cr), Cd, and zinc (Zn), in soils and water [7,8]. The interactions between metal ions and the biochar surface are related to complexation reactions and ion exchange, precipitation, and surface adsorption mechanisms [9,10]. The adsorption of heavy metal ions by biochar is reversible via non-electrostatic physical adsorption with weak affinities. Biochars derived from different raw materials and with different pyrolysis parameters (such as temperature, heating rate, and residence time, etc.) normally show different adsorption capacities for different metals [11–13]. For example, biochar derived from swine manure digestate had an 83.98% removal efficiency for As (III) [11]; and biochar derived from olive mill solid waste can remove > 80% of the lead and copper [12]. Therefore, new materials should be investigated, especially solid wastes, as raw materials in the preparation of biochars that could be used for heavy metal stabilization and immobilization.

The development of forestry planting and related industries has led to the creation of large amounts of forestry residues. However, little attention has been paid to the disposal of these forestry residues, which has led to resource waste and a potential ecological problem. The conversion of forest wood into biochar is a useful way of reusing forest wood waste. However, previous research on the adsorption-reduction process was not systematic and comprehensive. Therefore, the Cd adsorption capacity of biochar derived from woody and bamboo plants needs to be investigated.

In this study, a number of biochars were prepared by pyrolyzing 11 potential biochar materials at 600°C. The materials were either woody plants or bamboo, which were widely planted across EnShi in the mid-west forest land of China. The three biochar types with the highest adsorption capacity for Cd²⁺ were selected for further investigation. This study examined the Cd removal capacity, potential adsorption mechanism, and the kinetics of these biochars.

2. Materials and methods

2.1. Materials

Eleven types of wood chips (chestnut tree, poplar tree, wild cherry tree, *Rhus chinensis*, cedarwood, ginkgo tree, cedrela, *Pinus massoniana*, *Eucommia ulmoides* tree, walnut tree, and bamboo) were selected as raw materials for biochar preparation. The samples were collected from Enshi Forest Nature Reserve, which is located in mid-west China. The crushed materials were washed to remove impurities and then dried to constant weight at 80°C.

2.2. Preparation and selection of the best biochars

The biochars produced by the plants were first put into ceramic crucible with a lid and then heated in a muffle furnace to 600°C for 4 h. Then, the hot products were cooled to room temperature and ground into a fine powder.

The 11 types of biochar were added to Cd(NO₃)₂ solution at a concentration of 2 g/L. The mixture samples were then shaken in a water-bath set to a constant temperature of 25°C and vibrated at 120 rpm for 2 h. Following this, the samples were centrifuged at 5000 rpm and filtered through a 0.45 μm membrane. The Cd²⁺ concentration was detected by Atomic Absorption Spectroscopy (AAs). All the experiments were performed in triplicate.

The three biochars with the highest Cd²⁺ removal rates were selected for further investigation.

2.3. Batch equilibrium experiment

The optimal dosage and pH were measured using a batch equilibrium experiment. The biochars were added to 20 mg/L Cd(NO₃)₂ solution at concentrations of 0.2 g/L, 0.5 g/L, 1 g/L, 2 g/L, 3 g/L, 4 g/L, 5 g/L, 6 g/L, or 7 g/L. The solution pH values ranged from 2.0 to 9.0 with an interval value of 1.0. The mixture samples were shaken at 120 rpm and 25°C for 2 h. Then, the mixtures were centrifuged at 5000 rpm and filtered through a 0.45 μm membrane for Cd²⁺ analysis by AAs. All the experiments were performed in triplicate.

The isoelectric point of the biochar was determined from the ΔpH values. The initial pH values of the NaCl solution (20 mL of 0.01 mol/L solution) were moderated by NaOH or HCl solution so that they ranged between about pH 2.0 and 9.0. Then, 0.01 g of the each of the three biochars was added to the above NaCl solution. The mixture was heated to 30°C and shaken at 150 rpm for 24 h to ensure that the reaction was sufficient. The pH values analysis was performed in triplicate.

2.4. Adsorption kinetics

The adsorption kinetics were measured using a batch equilibrium experiment. The three biochars were each added to 20 mg/L Cd(NO₃)₂ solution, and the optimum dosage and pH were selected. The mixture samples were shaken at 25°C and 120 rpm for 5, 10, 15, 20, 30, 40, 50, 60, 80, 100, or 120 min. Then, the mixtures were centrifuged at 5000 rpm and filtered through a 0.45 μm membrane for Cd²⁺ analysis by AAs. All experiments were performed in triplicate.

2.5. Adsorption isotherms

The adsorption isotherms were determined using batch adsorption at a constant temperature (25°C), with mechanical shaking (~120 rpm), and a contact time of 1 h. The initial Cd²⁺ concentrations ranged between 5 and 60 mg/L, which were prepared by diluting the stock solution (1.0 g/L Cd²⁺). The three biochars were each added to the Cd²⁺ solution at the optimal biochar dosages and pH values. Then, the mixtures were centrifuged at 5000 rpm and filtered through a 0.45 μm membrane for Cd²⁺ analysis by AAs. All experiments were performed in triplicate. The adsorption capacity and removal efficiency were calculated from the following equations [14]:

$$Q_e = V \frac{(C_o - C_e)}{m} \quad (1)$$

$$R = 100\% * \frac{(C_0 - C_e)}{C_0} \quad (2)$$

where, Q_e is adsorption capacity (mg/g); C_0 is the initial solution concentration (mg/L); C_e is the equilibrium solution concentration (mg/L); V is the solution volume (L); and m is the biochar mass (g).

2.6. Sample characterization

The biochar was mixed with mono crystal KBr (CAS:7758-02-3, SP grade, Aladdin) in a 1/100 m/m ratio and was tableted. The tablets were analyzed by a Fourier transform infrared spectrophotometer (FTIR, VERTEX 70, Bruker) in the 4000–400 cm^{-1} wavenumber range so that the surface functional groups could be determined. A scanning electron microscope (SEM) was used to analyze the biochar micro structure. The biochar had previously been coated with a gold palladium film.

3. Results and discussion

3.1. Biochar selection

Fig. 1 shows Cd^{2+} adsorption onto the 11 types of biochar. It shows that the Cd^{2+} removal efficiencies varied greatly depending on the biochar type. The W-Biochar (biochar derived from walnut trees), C-Biochar (biochar derived from wild cherry trees) and B-Biochar (biochar derived from bamboo) had the best adsorption capacities with removal efficiencies of over 90% (initial Cd^{2+} concentration 2 g/L).

3.2. Biochar characterization

3.2.1 Fourier transform infra-red spectroscopy results

The FTIR spectra for B-Biochar, W-Biochar, and C-Biochar are shown in Fig. 2. The three biochar types had IR absorption peaks at 3431 cm^{-1} and 1383 cm^{-1} , and

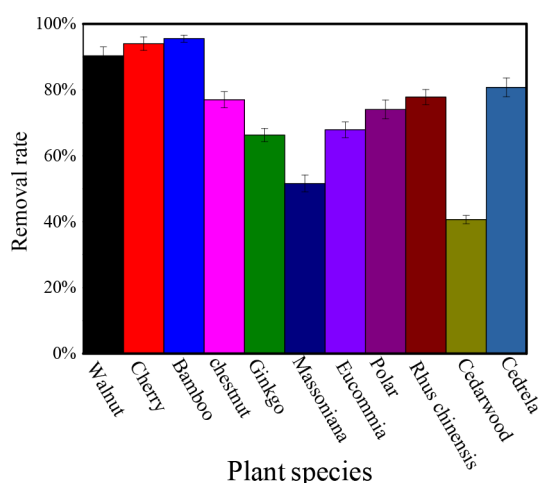


Fig. 1. The removal efficiencies of biochar on Cd^{2+} , experimented at biochar dosage 2 g/L, and Cd^{2+} concentration 20 mg/L.

a pointed shape. The 3431 cm^{-1} peak was assigned to the free –OH stretching vibration and the 1383 cm^{-1} peak was attributed the X-Y stretching vibration (δ as C-O), which was assigned to C-O in carboxylate [15]. These results indicated that the biochar surface was rich in hydroxyl and carboxyl groups. The carboxyl group could help retain toxic metals, which is crucial for metal sorption or stabilization [16–18]. Furthermore, the precipitation and surface complexation of Cd^{2+} with phenolic hydroxyl was also responsible for Cd^{2+} removal [19]. The highly conjugated aromatic structure may also compound with cations through the formation of cation- π [20–23], which depends on aromatization of the biochar surface. In this situation, adsorption was less affected by the surface charge of the biochar and the solution pH values. Therefore, it can be concluded that these three types of biochar, which contain hydroxyl and carboxyl groups, are suitable for Cd^{2+} adsorption.

3.2.2. Scanning electron microscope results

The SEM morphologies of the three biochars are shown in Fig. 3. The results suggest that the B-Biochar surface had more pore structures and adsorption active sites than the W-Biochar and C-Biochar. These differences meant that B-Biochar had a higher adsorbing capacity than the others, which was in accordance with Fig. 1. The surface morphology of the C-Biochar showed that it was composed of a regular texture grooved structure with a few small sized pores. The C-Biochar surface was more regular and smoother than the other two biochars. The whole surface of the W-Biochar was uneven and irregular with a plurality of melt-adhesion phenomena. This resulted in less effective adsorption and was consistent with the previous experimental observations (section 3.1).

3.3. Adsorption optimization

3.3.1. Dosage effects

The effects of dosage on biochar adsorption performance are shown in Fig. 4. The results showed that Cd^{2+} removal efficiencies gradually rose as the biochar dosage increased when it was below 2 g/L. At higher dosages, it tended to be a flat curve, and the removal rates no longer increased as the biochar dosage increased. One possible

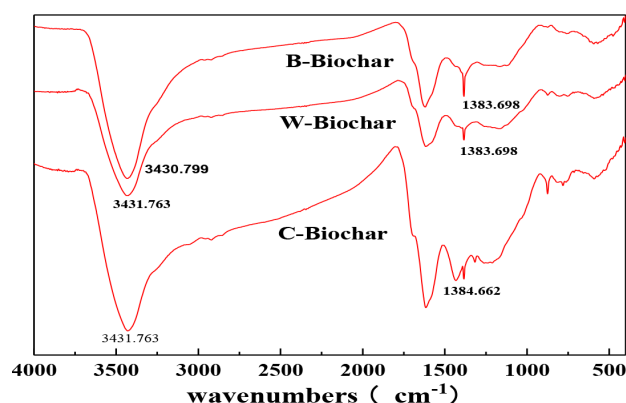


Fig. 2. Biochar infrared spectra.

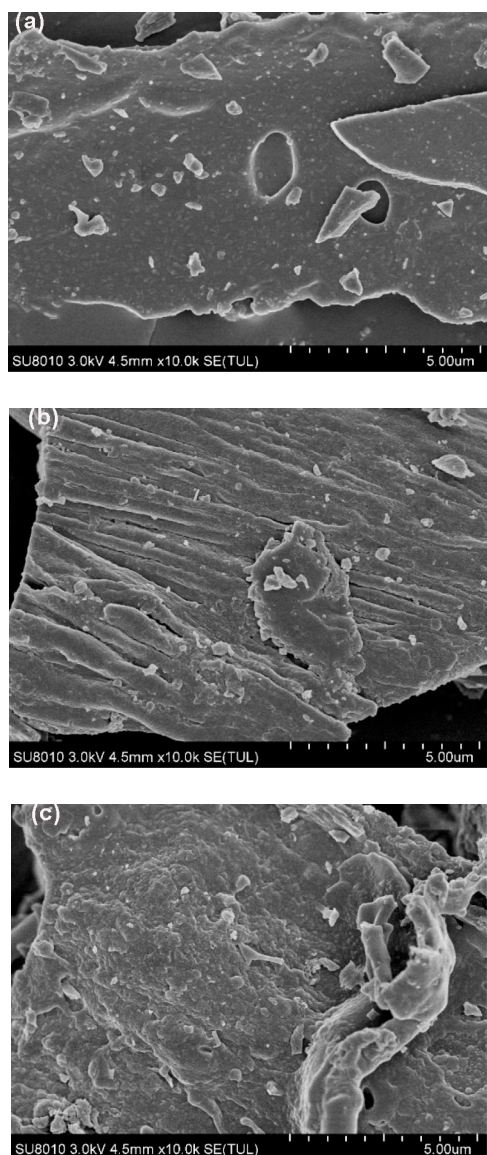


Fig. 3. (A) B-Biochar SEM; (B) C-Biochar SEM; (C) W-Biochar SEM.

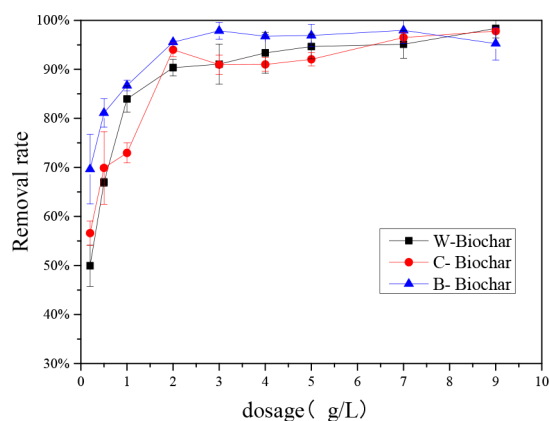


Fig. 4. Biochar dosage effects on Cd removal, experimented at Cd^{2+} concentration 20 mg/L.

reason could be that when the amount of biochar added was small, the total amount of active adsorption sites on the surface that could bind Cd^{2+} was low and tended to be saturated. The removal efficiencies of the B-Biochar, W-Biochar, and C-Biochar were 95.6%, 90.3%, and 94.0%, respectively when the concentration was 2 g/L. The adsorption efficiency of the three biochars for Cd^{2+} varied and followed the order: B-Biochar > C-Biochar > W-Biochar. In general, the results showed that the optimal dosage for the three biochars was 2 g/L.

3.3.2. Effect of pH value

The pH value is one of the most critical parameters for Cd^{2+} sorption because it influences the surface charge, ionization degree, and speciation of the pollutant [24]. The effects of pH on Cd^{2+} adsorption are shown in Fig. 5. The results showed that the removal efficiencies of B-Biochar and W-Biochar increased as the initial pH rose from 2.0 to 4.0, and the removal rate of C-Biochar rose as the initial pH increased from 2.0 to 6.0. Therefore, the results suggest that the optimal pH value for Cd^{2+} adsorption was 5.0 in this study. Similar acidic conditions were suitable for biochar produced from corn stover [25].

Cadmium predominantly exists as $\text{Cd}(\text{OH})_2$ at $\text{pH} > 8$, $\text{Cd}(\text{OH})^+$ at $\text{pH} 7.0\text{--}8.0$, and as Cd^{2+} at $\text{pH} < 7$ [26] (Fig. 6). At lower pHs, the Cd exists as free Cd^{2+} ions with soft acid characteristics, which are more likely to interact with the carboxyl groups because they are soft bases. This enhances the adsorption capacity. However, the higher concentration and mobility of H^+ ions in solution means that they compete with the Cd^{2+} for activated sites on the adsorbent. This leads to the transformation of carboxyl and hydroxyl groups into $-\text{COOH}$ and $-\text{OH}$, which decreases metal ion adsorption. As the pH increases, the H^+ concentration decreases and more negative active sites are available, which leads to the increased adsorption of Cd^{2+} species. At pH values above 7.0, the Cd species are predominantly $\text{Cd}(\text{OH})^+$ and $\text{Cd}(\text{OH})_2$. However, the removal efficiency by precipitation increases as the adsorption removal efficiency decreases [27], which means that ion exchange and the complex formation process are the major mechanisms for Cd removal. In this case, the Cd^{2+} is removed from the solution by

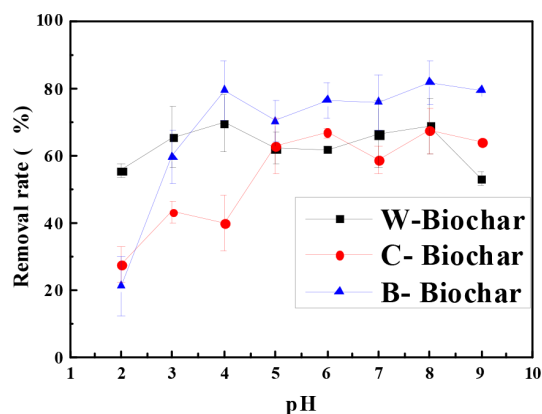


Fig. 5. Effect of initial pH value on Cd^{2+} removal, experimented at biochar dosage 2 g/L, and Cd^{2+} concentration 20 mg/L.

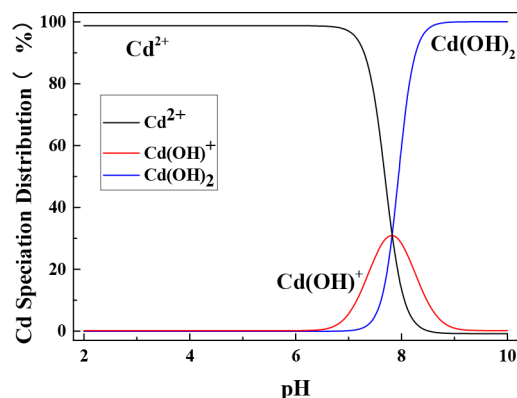


Fig. 6. Cadmium speciation distribution in aqueous solutions.

adsorption as well as by precipitation. Therefore, an optimum initial pH of 5.0 was chosen to perform all subsequent adsorption experiments.

The pH_{zpc} of an adsorbent is an important parameter, and the adsorbent surface is electrically neutral at the pH_{zpc} point. The relationship between initial pH and ΔpH is shown in Fig. 7. The pH_{zpc} values for W-Biochar, C-Biochar, and B-Biochar were 4.85, 4.68, and 5.32, respectively. Changes in the solution pH could influence the electrostatic interaction between Cd complexes and the adsorbent [28]. When the $\text{pH} < \text{pH}_{\text{pzc}}$, the biochar surface was protonated. This meant that there was greater electrostatic repulsion of the positively charged Cd^{2+} . When $\text{pH} > \text{pH}_{\text{pzc}}$, the surface was deprotonated and the electrostatic attraction between biochar and Cd^{2+} resulted in an enhanced adsorption capacity. Therefore, The results indicated that electrostatic interactions, precipitation, and coordination might be involved in Cd^{2+} adsorption onto biochar.

3.4. Kinetics and adsorption isotherms

3.4.1. Kinetics of the different biochars

The kinetic equation for the adsorption process can be used to describe the adsorption rate. The data could be fitted by a kinetic model that can then be used to investigate the adsorption mechanism. In this study, the following two models were used to determine the kinetics of the Cd^{2+} adsorption process:

1. The linear forms of the pseudo-first-order kinetic model was expressed as described in [29]:

$$\log(q_e - q_t) = \log q_e - \frac{k_1}{2.303} t \quad (3)$$

where k_1 is the rate constant of the pseudo-first-order kinetic model, ($1/h$) and q_t represents the adsorption uptake capacity at time t (mg/g).

2. The pseudo-second-order kinetic model was expressed in linear form by Eq. (4), as described in [29]:

$$\frac{t}{q_t} = \frac{1}{k_2 q_e^2} + \frac{1}{q_e} t \quad (4)$$

where k_2 is the adsorption rate constant ($\text{g}/(\text{mg}\cdot\text{h})$).

Table 1
Kinetic parameters for Cd^{2+} adsorption onto biochar

Kinetic parameters	B-Biochar	W-Biochar	W-Biochar
$q_{e,exp}$	8.60	8.47	7.94
Pseudo-first-order kinetics	$q_{e,cal}$ 7.56	6.24	6.24
	k_1 0.127	0.103	0.103
	R^2 0.8848	0.8948	0.8948
Pseudo-second-order kinetics	$q_{e,cal}$ 8.5984	7.9302	7.9302
	k_2 0.043	0.321	0.321
	R^2 0.999	0.999	0.999

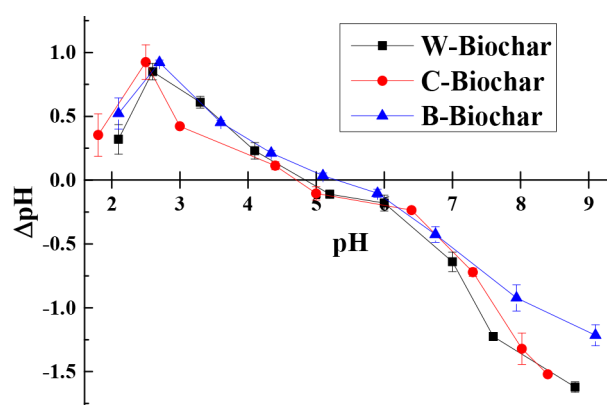


Fig. 7. Relationship between the initial pH and ΔpH values.

The kinetic fitting data is shown in Table 1. The results showed that the pseudo-second-order model gave a higher correlation coefficient (R^2) than the pseudo-first-order model (Fig. 8). The $q_{e,cal}$ (calculated adsorption capacity) was closer to $q_{e,exp}$ (experimental adsorption capacity) with a relative error below 1%. Therefore, the adsorption process could be described by the pseudo-second-order rather than the pseudo-first-order kinetic model. The pseudo-second-order kinetic model was based on the assumption that the adsorption rate was controlled by a chemisorption mechanism. The mechanism involves the sharing or transfer of electron pairs between the adsorbent. It has been reported that the Cd^{2+} is attached to the biochar surface by a chemisorption mechanism [30]. Therefore, the results indicated that the chemical process might be the rate-limiting step in the Cd^{2+} adsorption process.

Fig. 9 shows that the biochar had a fast adsorption effect on Cd^{2+} , and the majority of Cd^{2+} in solution was adsorbed in the first 20 min. This was the rapid adsorption stage. During this stage, the Cd^{2+} removal efficiencies were more than 80%. Between 20–40 min, removal efficiencies increased slowly. Therefore, this stage is called the slow adsorption stage. Above 40 min, adsorption equilibriums were achieved and the removal efficiencies no longer increased. The adsorption process might be described as follows: (1) The Cd^{2+} was initially adsorbed onto the outer surface of the biochar. (2) Then, the adsorbate gradually moved from the macropores into micropores via transition holes, which meant that the Cd^{2+} transfer rate gradually decreased in the inner pores.

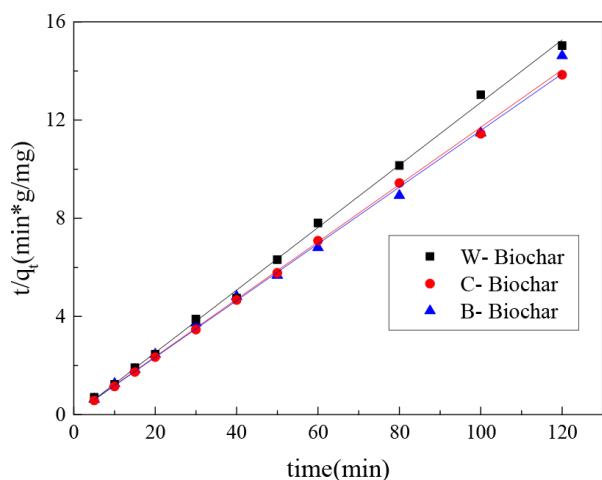


Fig. 8. Adsorption pseudo-secondary kinetics model.

(3) Finally, the adsorption capacity slowly increased until the adsorption equilibrium point was reached.

3.4.2. Adsorption isotherms

The relationship between Cd²⁺ equilibrium concentrations and adsorption capacities are shown in Fig. 10. The results indicated that the adsorption capacity increased as the initial Cd²⁺ concentration rose. When the Cd²⁺ reached an equilibrium concentration, the adsorption capacity remained basically unchanged.

In this study, the Langmuir Eq. (5) and Freundlich Eq. (6) were used to fit the experimental data. The Langmuir equation is a theoretical derivation formula, and the Freundlich equation is a pure empirical formula expressed in the form of an exponential adsorption isotherm [31,32]:

$$Q_e = \frac{q_m b C_e}{1 + b C_e} \quad (5)$$

$$Q_e = K_F C_e^{1/n} \quad (6)$$

where q_m is the maximum adsorption capacity, which is an important indicator of adsorption performance (mg/g); b is the Langmuir adsorption characteristic constant and shows the relationship between the adsorbent and the adsorbate (L/g). The adsorption affinity increases at higher b values. K_F is a parameter of Freundlich adsorption capacity and n is an empirical parameter that describes the adsorption strength, which is directly related to the heterogeneity of the adsorbents.

Figs. 11 and 12 show that the equilibrium data were better simulated by the Langmuir isotherm than the Freundlich isotherm because it had higher R² values. This suggested that monolayer chemisorption of Cd²⁺ might occur on homogeneous biochar surfaces. The maximum equilibrium adsorption capacities derived from the Langmuir model were 16.85 mg/g, 10.62 mg/g, and 21.45 mg/g for C-Biochar, W-Biochar, and B-Biochar, respectively. The results were consistent with the experimental values.

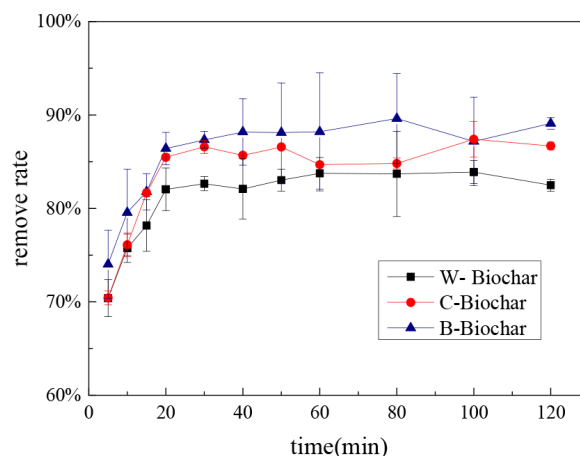


Fig. 9. Effect of time on Cd removal, experimented, experimented at dosage 2 g/L, pollutant concentration 20 mg/L and pH 5.

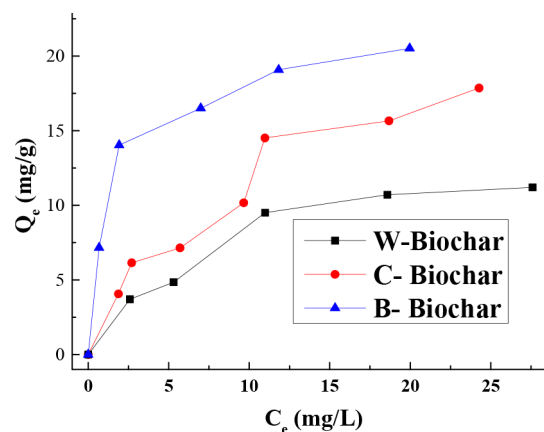
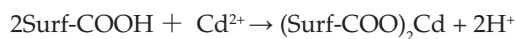
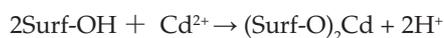


Fig. 10. Relationship between equilibrium concentration and adsorption capacity, experimented at dosage 2 g/L, pollutant concentration 20 mg/L and pH 5.

3.5. Potential mechanisms

Adsorption capacity is affected by the number of activated sites [33]. It increases as the Cd²⁺ concentration rises and gradually reaches an upper adsorption limit asymptote because of the limited number of sorption sites on the biochar surfaces [34]. At low Cd²⁺ concentrations, the activated sites are relatively abundant, which leads to increased Cd²⁺ attachment. In contrast, Cd²⁺ removal efficiency starts to fall at higher levels due to the lack of available adsorption sites. Surface morphology directly affected the number of active sites on the biochar surfaces and it was reason that caused the differences in the adsorption capacities of the three biochars.

Ion exchange is an important Cd²⁺ biochar adsorption mechanism [35] and can be expressed as follows [36]:



The ion exchanges that took place were between positively charged Cd²⁺ and negatively charged groups in

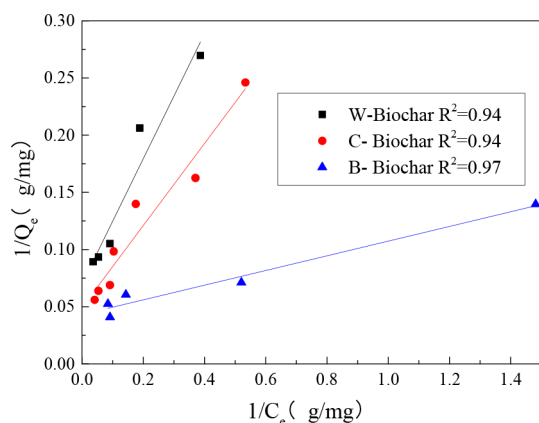


Fig. 11. Langmuir isotherm fitting.

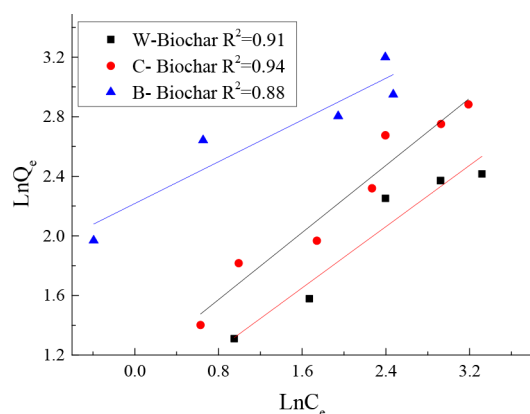


Fig. 12. Freundlich isotherm fitting.

Table 2
Adsorption isotherm fitting parameters

Materials	Langmuir isotherm fitting			Freundlich isotherm fitting		
	R ²	<i>b</i>	<i>Q_m</i>	R ²	<i>K_F</i>	<i>n</i>
C-Biochar	0.94	0.049	20.33	0.94	1.63	1.78
W-Biochar	0.94	0.070	14.29	0.91	2.29	1.94
B-Biochar	0.97	0.043	23.20	0.88	9.18	2.85

the biochar structure, which is a non-specific adsorption process with low energy requirements [37]. Solution pH is an important factor in the ion exchange process. Higher H^+ concentrations prevents the deprotonation process in highly acidic environments. Furthermore, $Cd(OH)^+$ and $Cd(OH)_2$ become the dominant species at high pH levels, and optimum adsorption is not reached in the above pH range [38]. Therefore, electrostatic interactions, precipitation and coordination might be responsible for Cd^{2+} adsorption onto biochar, whereas ion exchange might be the main mechanism at pH 5. The highly conjugated aromatic structure may also compound with cations through the formation of cation- π , which could promote the adsorption progress. The kinetics analysis suggests that the chem-

ical process might be the rate-controlling step in the Cd^{2+} adsorption process.

4. Conclusions

Biochars derived from the woody plants and bamboo investigated in this study could be used to remove Cd^{2+} . The optimal adsorption conditions were a biochar dosage of 2g/L and pH = 5.0. The Cd^{2+} adsorption performance order for the three best performing biochars was B-Biochar > C-Biochar > W-Biochar, and the adsorption process conformed to the pseudo-second-order kinetic model. It took 40 minutes to reach adsorption equilibrium, and isothermal adsorption could be described by the Langmuir isotherm equation with maximum adsorption capacities of 15.81 mg/g, 9.83 mg/g, and 19.46 mg/g for C-Biochar, W-Biochar, and B-Biochar, respectively. The hydroxyl and carboxyl functional groups, and the special micropore structure suggested that biochar derived from woody plants or bamboo are promising materials that could be used to ameliorate Cd^{2+} contamination.

Acknowledgements

This work was supported by the National Natural Science Foundation of China (Grant Nos. 41501537 and 41571306), the Hubei Key Laboratory for Efficient Utilization and Agglomeration of Metallurgic Mineral Resources (Grant No. 2017zy003), and the Project of Excellent Fund in Hubei (Grant Nos. 2018CFA067 and 2017zy003).

References

- [1] L. Jiang, W. Wang, Z. Chen, Q. Gao, Q. Xu, H. Cao, A role for *apx1* gene in lead tolerance in *Arabidopsis thaliana*, *Plant Sci.*, 256 (2017) 94–102.
- [2] K. Li, J. Chen, P. Jin, J. Li, J. Wang, Y. Shu, Effects of Cd accumulation on cutworm *Spodoptera litura* larvae via Cd treated Chinese flowering cabbage *Brassica campestris* and artificial diets, *Chemosphere*, 200 (2018) 151–163.
- [3] M.A. Khan, S. Khan, A. Khan, M. Alam, Soil contamination with cadmium, consequences and remediation using organic amendments, *Sci. Total Environ.*, 601–602 (2017) 1591–1605.
- [4] X. Cui, S. Fang, Y. Yao, T. Li, Q. Ni, X. Yang, Z. He, Potential mechanisms of cadmium removal from aqueous solution by *Canna indica* derived biochar, *Sci. Total Environ.*, 562 (2016) 517–525.
- [5] B. Song, G. Zeng, J. Gong, P. Zhang, J. Deng, C. Deng, J. Yan, P. Xu, C. Lai, C. Zhang, M. Cheng, Effect of multi-walled carbon nanotubes on phytotoxicity of sediments contaminated by phenanthrene and cadmium, *Chemosphere*, 172 (2017) 449–458.
- [6] M.K. Hossain, V. Strezov, K.Y. Chan, A. Ziolkowski, P.F. Nelson, Influence of pyrolysis temperature on production and nutrient properties of wastewater sludge biochar, *J. Environ. Manage.*, 92(1) (2011) 223–228.
- [7] M. Ahmad, A.U. Rajapaksha, J.E. Lim, M. Zhang, N. Bolan, D. Mohan, M. Vithanage, S.S. Lee, Y.S. Ok, Biochar as a sorbent for contaminant management in soil and water: a review, *Chemosphere*, 99(3) (2014) 19–33.
- [8] J.A. Ippolito, K.A. Spokas, J.M. Novak, R.D. Lentz, K.B. Cantrell, Biochar elemental composition and factors influencing nutrient retention, *Biochar for Environmental Management Science Technology, Implementation*, (2015).

- [9] L. Beesley, M. Marmiroli, The immobilisation and retention of soluble arsenic, cadmium and zinc by biochar, *Environ Pollut.*, 159(2) (2011) 474–480.
- [10] A. Méndez, A. Gómez, J. Paz-Ferreiro, G. Gascó, Effects of sewage sludge biochar on plant metal availability after application to a Mediterranean soil, *Chemosphere*, 89(11) (2012) 1354–1359.
- [11] B. Jiang, Y. Lin, J.C. Mbog, Biochar derived from swine manure digestate and applied on the removals of heavy metals and antibiotics, *Bioresour Technol.*, 270 (2018) 603–611.
- [12] S.O. Abdelhadi, C.G. Dosoretz, G. Rytwo, Y. Gerchman, H. Azaizeh, Production of biochar from olive mill solid waste for heavy metal removal, *Bioresour Technol.*, S0960852417313184. (2017)
- [13] M. Luo, H. Lin, B. Li, Y. Dong, Y. He, L. Wang, A novel modification of lignin on corncob-based biochar to enhance removal of cadmium from water, *Bioresour Technol.*, 259 (2018) 312–318.
- [14] S. Sugashini, Performance of ozone treated rice husk carbon (OTRHC) for continuous adsorption of Cr (VI) ions from synthetic effluent, *J. Environ. Chem. Eng.*, 1 (2013) 79–85.
- [15] X. Zhang, W.J. Fu, Y.X. Yin, Z.H. Chen, R.L. Qiu, M.O. Simonnot, X.F. Wang, Adsorption-reduction removal of Cr(VI) by tobacco petiole pyrolytic biochar: batch experiment, kinetic and mechanism studies, *Bioresour Technol.*, 268 (2018) 149–157.
- [16] Z. Chen, X. Xiao, B. Chen, L. Zhu, Quantification of chemical states, dissociation constants and contents of oxygen-containing groups on the surface of biochars produced at different temperatures, *Environ. Sci. Technol.*, 49(1) (2015) 309–317.
- [17] Q. Linbo, C. Baoliang, Dual role of biochars as adsorbents for aluminum: the effects of oxygen-containing organic components and the scattering of silicate particles, *Environ. Sci. Technol.*, 47(15) (2013) 8759–8768.
- [18] M. Uchimiya, I.M. Lima, K.T. Klasson, S.C. Chang, L.H. Wartelle, J.E. Rodgers, Immobilization of heavy metal ions (Cu(II), Cd(II), Ni(II), and Pb(II)) by broiler litter-derived biochars in water and soil, *J. Agric. Food Chem.*, 58(9) (2010) 5538–5544.
- [19] R.Z. Wang, D.L. Huang, Y.G. Liu, C. Zhang, C. Lai, G.M. Zeng, M. Cheng, X.M. Gong, J. Wan, H. Luo, Investigating the adsorption behavior and the relative distribution of Cd²⁺, sorption mechanisms on biochars by different feedstock, *Bioresour Technol.*, 261 (2018) 265–271.
- [20] M.J. Antal, M. Grønli, The art, science, and technology of charcoal production, *Ind. Eng. Chem. Res.*, 42(8) (2003) 1619–1640.
- [21] H.P. Boehm, Some aspects of the surface chemistry of carbon blacks and other carbons, *Carbon*, 32(5) (1994) 759–769.
- [22] J. Sunner, K. Nishizawa, P. Kebarle, Ion-solvent molecule interactions in the gas phase the potassium ion and benzene, *J. Phys. Chem.*, 85(13) (1981).
- [23] K.D. Daze, F. Hof, The cation- π interaction at protein-protein interaction interfaces: developing and learning from synthetic mimics of proteins that bind methylated lysines, *Accounts Chem. Res.*, 46(4) (2013) 937–945.
- [24] F. Debela, R.W. Thring, J.M. Arocena, Immobilization of heavy metals by co-pyrolysis of contaminated soil with woody biomass, *Water Air Soil Poll.*, 223(3) (2012) 1161–1170.
- [25] X. Deng, H. Zhou, X.N. Qu, Optimization of Cd(II) removal from aqueous solution with modified corn straw biochar using Plackett-Burman design and response surface methodology, *Desal. Water Treat.*, 70 (2017) 210–219.
- [26] R. Leyva-Ramos, J.R. Rangel-Mendez, J. Mendoza-Barron, L. Fuentes-Rubio, R.M. Guerrero-Coronado, Adsorption of cadmium(II) from aqueous solution onto activated carbon, *Water Sci. Technol.*, 35(7) (1997) 205–211.
- [27] J.H. Huang, F. Yuan, G.M. Zeng, X. Li, Y.L. Gu, L.X. Shi, W.C. Liu, Y.H. Shi, Influence of pH on heavy metal speciation and removal from wastewater using micellar-enhanced ultra filtration, *Chemosphere*, 173 (2017) 199–206.
- [28] M.W. Yap, N.M. Mubarak, J.N. Sahu, E.C. Abdullah, Microwave induced synthesis of magnetic biochar from agricultural biomass for removal of lead and cadmium from wastewater, *J. Ind. Eng. Chem.*, (2016).
- [29] M. Doğan, M.H. Karaoğlu, M. Alkan, Adsorption kinetics of maxilon yellow 4gl and maxilon red grl dyes on kaolinite, *J. Hazard. Mater.*, 165(1–3) (2009) 1142–1151.
- [30] N. Zhou, H. Chen, J. Xi, D. Yao, X. Lu, Biochars with excellent Pb(II) adsorption property produced from fresh and dehydrated banana peels via hydrothermal carbonization, *Bioresour. Technol.*, 232 (2017) 204–210.
- [31] I. Langmuir, The constitution and fundamental properties of solids and liquids, *J. Franklin I.*, 184(5) (1916) 102–105.
- [32] K.G. Bhattacharyya, S.S. Gupta, Influence of acid activation on adsorption of Ni(II) and Cu(II) on kaolinite and montmorillonite: Kinetic and thermodynamic study, *Chem. Eng. J.*, 136(1) (2008) 1–13.
- [33] Ahmedzeki, S. Nada, Adsorption filtration technology using iron-coated sand for the removal of lead and cadmium ions from aquatic solutions, *Desal. Water Treat.*, 51(28–30) (2013) 5559–5565.
- [34] S.E. Elaigwu, V. Rocher, G. Kyriakou, G.M. Greenway, Removal of Pb²⁺ and Cd²⁺ from aqueous solution using chars from pyrolysis and microwave-assisted hydrothermal carbonization of prosopis africana shell, *J. Ind. Eng. Chem.*, 20(5) (2014) 3467–3473.
- [35] H.H. Cho, K. Wepasnick, B.A. Smith, F.K. Bangash, D.H. Fairbrother, W.P. Ball, Sorption of aqueous Zn [II] and Cd [II] by multiwall carbon nanotubes: the relative roles of oxygen-containing functional groups and graphenic carbon, *Langmuir*, 26(2) (2010) 967–981.
- [36] L.I. Li, L.U. Yu-Chao, L. Ya, S. Hong-Wen, L. Zhong-Yao, Adsorption mechanisms of cadmium (II) on biochars derived from corn straw, *J. Agro-Environ. Sci.*, 31(11) (2012) 2277–2283.
- [37] M. Eve, BAZINET, Laurent, Ion-exchange membrane fouling by peptides: a phenomenon governed by electrostatic interactions, *J. Membr. Sci.*, 369 (2011) 359–366.
- [38] B. Reed, M. Matsumoto, Modeling cadmium adsorption by activated carbon using the Langmuir and Freundlich isotherm expressions, *J. Sep. Sci.*, 28(13–14) (1993) 17.